Negative Feedback Synchronizes Islets of Langerhans

Raghuram Dhumpa,[†] Tuan M. Truong,[†] Xue Wang,[†] Richard Bertram,[‡§*] and Michael G. Roper[†§*]
[†]Department of Chemistry and Biochemistry, Florida State University, Tallahassee, FL 32306; [‡]Department of Mathematics and Program in Neuroscience, Florida State University, Tallahassee, FL 32306; and [§]Program in Molecular Biophysics, Florida State University, Tallahassee, FL 32306

ABSTRACT Insulin is released from the pancreas in pulses with a period of ~ 5 min. These oscillatory insulin levels are essential for proper liver utilization and perturbed pulsatility is observed in type 2 diabetes. What coordinates the many islets of Langerhans throughout the pancreas to produce unified oscillations of insulin secretion? One hypothesis is that coordination is achieved through an insulin-dependent negative feedback action of the liver onto the glucose level. This hypothesis was tested in an in vitro setting using a microfluidic system where the population response from a group of islets was input to a model of hepatic glucose uptake, which provided a negative feedback to the glucose level. This modified glucose level was then delivered back to the islet chamber where the population response was again monitored and used to update the glucose concentration delivered to the islets. We found that, with appropriate parameters for the model, oscillations in islet activity were synchronized. This approach demonstrates that rhythmic activity of a population of physically uncoupled islets can be coordinated by a downstream system that senses islet activity and supplies negative feedback. In the intact animal, the liver can play this role of the coordinator of islet activity.

INTRODUCTION

Islets of Langerhans secrete insulin in response to elevations in the blood glucose level. As with many endocrine systems, insulin secretion from the pancreas is pulsatile, yielding ~ 5 min oscillations in the plasma insulin concentration (1–3). These oscillations are important, because pulsatile insulin levels in the portal vein are more effective than constant levels at evoking insulin action in the liver (3), and disorganized insulin pulsatility is observed in people with diabetes and their near relatives (4,5).

The activity of individual islets is also pulsatile, exhibiting a ~ 5 min period in electrical activity, intracellular Ca^{2+} concentration ($[Ca^{2+}]_i$), and insulin secretion (6). The similarity of the periods from individual islet activity and in vivo pulsatility suggests that the hundreds of thousands of islets scattered throughout the pancreas are synchronized. However, they are not physically coupled, so what coordinates their activity enabling the population of oscillators to produce a coherent rhythm in insulin secretion? Islet synchronization must occur, otherwise phase and period differences between the individual islet oscillators would result in an overall blood insulin level that is relatively flat. Yet pulsatile insulin levels have been observed in humans (1), mice (2), rats (7), dogs (8), and monkeys (9).

One mechanism for synchronization is that islets may be coordinated through intrapancreatic ganglia (10,11). The pancreas is innervated by preganglionic vegal neurons (12–15), and the ganglia have been shown to exhibit electrical excitability when autonomic nerve trunks were stimulated in the cat (16). It has been shown that a bolus of the cholinergic agonist carbachol can transiently synchronize islet oscillations (17), and application of a pulse of ATP induced a $[Ca^{2+}]_i$ response in islets, suggesting that release of ATP from ganglia neurons may help to coordinate islet activity (18). However, there is at present no data suggesting that ganglia neurons exhibit pacemaking activity, as would be required to synchronize the population of islets in the pancreas.

A study using mathematical modeling and computer simulations demonstrated that interactions between pancreatic islets and the liver would be sufficient to coordinate islet rhythmicity into 5 min pulses (19). According to this hypothesis (Fig. 1 *A*), insulin secreted from the pancreas would signal the liver to reduce hepatic glucose output and initiate glucose uptake, causing a reduction in blood glucose. The reduced glucose level would then be sensed by each islet in the population, lowering the collective insulin output from the pancreas. In this way, the liver acts as a negative feedback on the islets by reducing blood glucose levels. The lower insulin levels would then promote a reduced glucose uptake by the liver allowing the levels of glucose to rise again. These variable glucose levels act as the coordinating signal for islet activity promoting oscillations in both insulin and glucose. Although glucose uptake by other tissues, such as muscle, is quantitatively important, these tissues would be exposed to smaller amplitude changes in insulin levels than the liver (1).

This hypothesis of a dynamic insulin-glucose feedback system coordinating islet activity to produce coherent 5 min pulses of insulin was postulated some years ago (20–23), yet no experimental test of this theory has been described. Evidence for this hypothesis comes from

Submitted January 10, 2014, and accepted for publication April 11, 2014.
*Correspondence: bertram@math.fsu.edu or roper@chem.fsu.edu
Raghuram Dhumpa and Tuan M. Truong contributed equally to this work.
Editor: Daniel Beard

0006-3495/14/05/2275/8 $2.00
http://dx.doi.org/10.1016/j.bpj.2014.04.015

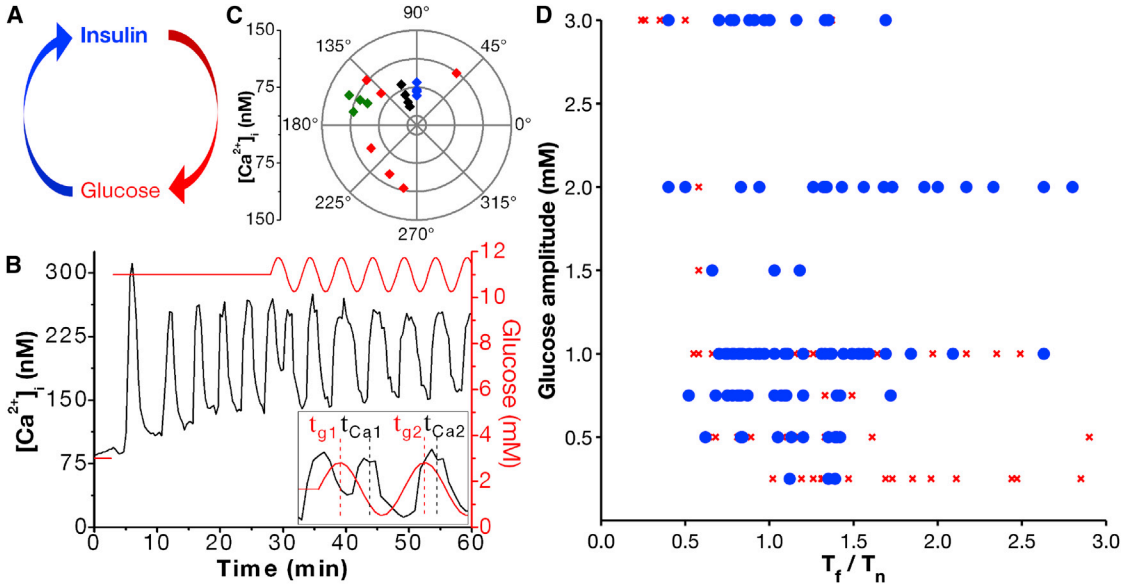

FIGURE 1 Mechanism of negative feedback and open-loop experiments. (*A*) Insulin released from the pancreas acts on the liver promoting glucose uptake. Lowered glucose levels reduces the secretion of insulin from the pancreas, allowing the glucose levels to rise again. This dynamic interaction would result in oscillations in both insulin and glucose levels. (*B*) Using a microfluidic system, 11 mM glucose (*red line*) was delivered to an islet of Langerhans and $[Ca^{2+}]_i$ was recorded using Fura-2 fluorescence (*black line*). At time 28 min, a sinusoidal glucose level was delivered with a 5 min period and 0.75 mM amplitude. Inset shows a zoomed-in view of the first two glucose and $[Ca^{2+}]_i$ oscillations. The phase angle (Φ) between the oscillations was measured using the times of the glucose oscillations (t_{g1}, t_{g2}) and times of the $[Ca^{2+}]_i$ oscillations (t_{Ca1}, t_{Ca2}) as described in (26). (*C*) Phase angles are displayed on a polar plot for successive oscillations from individual islets exposed to sinusoidal glucose with period and amplitude combinations of 5 min, 1 mM (*green*); 6.5 min, 1 mM (*black*); 8 min, 3 mM (*blue*); and 7 min, 0.25 mM (*red*). The radius of the point on the plot is the amplitude of the Ca^{2+} oscillation. The phase angles converged to a constant value for the green, black, and blue points, indicating entrainment of the islets to the oscillatory glucose. In the experiment shown by the red points, Φ did not converge, indicating a lack of entrainment. (*D*) Entrainment diagram in which the ratio of the glucose forcing period (T_f) to the natural period (T_n) of the islet oscillations is shown on the abscissa and the amplitude of the imposed glucose oscillations on the ordinate. The degree of entrainment is measured with the synchronization index (λ). A synchronization index value greater than or equal to 0.70 (high degree of entrainment) is shown as a blue circle and below as a red cross.

oscillations of insulin (1,2,7–9) and glucose (9,24) observed in vivo. In this report, a microfluidic system was used to perfuse a population of islets with glucose and the average response of the population was used to continuously update the glucose level. The updating was achieved with a simple mathematical model for negative feedback. Without the negative feedback, the islets exhibited uncoordinated oscillations in $[Ca^{2+}]_i$ and insulin secretion. When the feedback was turned on these oscillations quickly synchronized, producing glucose and insulin oscillations with periods of 5 to 8 min. These results indicate that a negative feedback on glucose levels can coordinate pulsatile insulin release.

MATERIALS AND METHODS

Chemicals and reagents

Potassium chloride (KCl), sodium chloride (NaCl), calcium chloride ($CaCl_2$), magnesium chloride ($MgCl_2$), dimethyl sulfoxide (DMSO), tricine, and penicillin-streptomycin were purchased from Sigma-Aldrich (Saint Louis, MO). Pluronic F-127 and fura 2 acetoxymethyl ester (fura 2-AM) were from Life Technologies (Grand Island, NY). Glucose (dextrose) was purchased from Thermo Fisher Scientific (Waltham, MA). RPMI 1640 was purchased from Mediatech (Manassas, VA). Gentamicin sulfate was purchased from Lonza (Basel, Switzerland). Collagenase P (from Clostridium histolyticum) was purchased from Roche Diagnostics (Indianapolis, IN). Poly(dimethylsiloxane) (PDMS) prepolymer (Sylgard 184) was purchased from Dow Corning (Midland, MI). All solutions were made with Milli-Q (Millipore, Bedford, MA) 18 MΩ cm deionized water.

Isolation and culture of islets of Langerhans

All experiments were performed under guidelines approved by the Florida State University Animal Care and Use Committee (ACUC) (protocol No. 1235). Islets of Langerhans were isolated from male CD-1 mice (30 – 50 g). Islets were isolated using collagenase P digestion as described previously (25–27). The isolated islets from multiple mice were mixed during picking and randomly chosen for the experiment. After isolation, islets were incubated at 37°C, 5% CO_2 in RPMI 1640 media containing 11 mM glucose, 10% calf serum, 100 units mL^{-1} penicillin, 100 μg mL^{-1} streptomycin, and 10 μg mL^{-1} gentamicin. Islets were used within five days after isolation and fresh media was provided on day 3 after isolation.

For $[Ca^{2+}]_i$ monitoring, 1.0 μL of 5.0 mM fura 2-AM in DMSO and 1.0 μL Pluronic F-127 in DMSO were mixed and transferred into 2 mL of RPMI to form a final fura 2-AM concentration of 2.5 μM. Each batch of islets was incubated in this solution at 37°C and 5% CO_2 for 40 min. After this time, the islets were removed and placed in the microfluidic device and rinsed with 3 mM glucose in balanced salt solution (BSS). The BSS was composed of 2.4 mM $CaCl_2$, 125 mM NaCl, 1.2 mM $MgCl_2$, 5.9 mM KCl, varying concentrations of glucose as described below, and 25 mM tricine at pH 7.4 and was used in all experiments.

Insulin quantification

Ten islets were used in the experiment described in the text and $[Ca^{2+}]_i$ was monitored as described below. During the experiment, perfusate was collected at 1 min intervals from the top of the chamber. An insulin ELISA (Ultra Sensitive Mouse Insulin ELISA kit, Crystal Chem, Inc., Downers Grove, IL) was used to quantify insulin levels according to the manufacturer's instructions.

Microfluidic device

A microfluidic device design was adapted from (28). The PDMS-glass hybrid device was fabricated using conventional photolithography. All channel dimensions were 250 × 40 μm (width × height). The device consisted of two inputs and three outputs. The inputs were connected to 60 mL syringes suspended by a pulley system. The syringes contained BSS described above with either 3 or 13 mM glucose. The height of one of the syringes was actuated by a stepper motor controlled by a LabVIEW (National Instruments, Austin, TX) program while the height of the other syringe was displaced in the opposite direction by an equal amount using a fixed-length belt and pulley system (28). The difference in the heights of the two syringes caused different flow rates of the two glucose solutions to enter the 70 mm mixing channel with excess buffer diverted via the side channels to a waste reservoir. This design maintains a constant total flow rate in the device. The buffers passing to the mixing channel were mixed to homogeneity and delivered to a 0.8 mm diameter chamber that housed 5 to 10 islets. By changing the heights of the two syringes, the concentration of glucose delivered to the islets could be changed. The system was calibrated in a manner similar to our previous reports (25–27). It took ~ 30 s for a new glucose concentration to be delivered to the islet chamber.

The microfluidic device was fixed on the stage of a Nikon Eclipse Ti inverted microscope. A lamp integrated with filter wheel and shutter (Lambda XL, Sutter Instruments, Novato, CA) containing appropriate filters was used for excitation of fura-2 at 340 and 380 nm. The images were acquired with a 150 ms exposure every 20 s using a CCD (Cascade, Photometrics, Tucson, AZ) controlled by Nikon NIS Elements software (Nikon, Melville, NY). The ratio of fluorescence intensity excited at 340 nm to that at 380 nm (F_{340}/F_{380}) for all islets were obtained by NIS software and exported to a file. The F_{340}/F_{380} ratio values were converted to $[Ca^{2+}]_i$ using predetermined calibration values that were found by standard methods (29). The LabVIEW program that controlled the syringes then read the $[Ca^{2+}]_i$ and calculated Ca_{avg} to be used in the feedback.

Mathematical model

The differential equation for the extracellular glucose concentration, Eq. 6, was discretized using the forward Euler method. Let $F(I^n_{avg}, G^n_e) = G_\infty(I^n_{avg}) - G^n_e/\tau_G$ be the right-hand side of the differential equation, where the superscript "n" represents "time step n." Then at each subsequent sampling point, G_e was updated from its previous value G^n_e to its new value G^{n+1}_e according to the following:

$$G^{n+1}_e = G^n_e + F\left(I^n_{avg}, G^n_e\right)\Delta t \qquad (1)$$

where $\Delta t = 1$ s was the time step. The Ca_{avg} and I_{avg} values were updated every 20 time steps.

Synchronization index (λ)

The synchronization index (λ) was calculated as described previously (25,30,31). Briefly, for a group of five islets, the $[Ca^{2+}]_i$ oscillations of the first islet are compared with the $[Ca^{2+}]_i$ oscillations of each of the remaining four islets, and in each case the degree of phase locking is captured as $\lambda_{1,j}$ for $j = 2,\ldots,5$. A λ value near 1 means that two $[Ca^{2+}]_i$ oscillation traces are nearly phase locked, whereas a λ near 0 means that they are not. The calculation is then repeated by comparing the $[Ca^{2+}]_i$ oscillations of islet 2 with each of the others, and computing $\lambda_{2,j}$ for $j = 1,3,4,5$. This is repeated three more times giving $\lambda_{3,j}$, $\lambda_{4,j}$, $\lambda_{5,j}$, and in the end an overall λ is calculated as the average of the 20 individual indices. For the open-loop experiments (Fig. 1 *D*), λ was calculated in a similar manner by computing the degree of phase locking between an individual islet and the glucose trace.

Data analysis

For calculation of synchronization index and oscillation periods described above, the initial 5 min of each F_{340}/F_{380} trace after a change in glucose level were not used for data analysis. For example, during an open-loop experiment, the timing of the glucose delivery was the following: t = 0 – 3 min, 3 mM glucose; t = 3 – 23 min, 11 mM glucose; t = 23 – 60 min, oscillatory glucose. To determine T_n and T_f, the F_{340}/F_{380} trace from 8 – 23 min and 28 – 60 min were used, respectively. This was performed to reduce transients in the $[Ca^{2+}]_i$ levels associated with the change in glucose level (25). T_n, T_f, and the period of $[Ca^{2+}]_i$ oscillations with sinusoidal glucose were calculated by fast Fourier transforms of the $[Ca^{2+}]_i$ trace with baseline subtracted.

Phase angle

In Fig. 1 *C*, the islet response to the forcing glucose signal was shown by a phase angle (Φ) between $[Ca^{2+}]_i$ oscillations and the glucose oscillations. Φ_i (for i = 1, 2, 3,…, n oscillations) was found by measuring the difference in the times of the midpoints between each glucose peak ($t_{g,i}$) and the closest $[Ca^{2+}]_i$ peak ($t_{c,i}$):

$$\Phi_i = 360^\circ\left(t_{c,i} - t_{g,i}\right)/T \qquad (2)$$

where T is the period of the forcing glucose wave. The radius of the point on the polar plot is the amplitude of the $[Ca^{2+}]_i$ oscillation.

RESULTS

Effects of oscillatory glucose levels on islets

A prediction of the hypothesis that a dynamic interaction between the pancreas and liver could synchronize an islet population is that the glucose levels sensed by islets will be oscillatory. Initial experiments were, therefore, first performed in an open-loop manner in which the glucose concentration was varied sinusoidally and the range of glucose amplitudes and periods that could effectively entrain islet activity was determined.

Glucose oscillations with periods from 5 to 10 min, a median value of 11 mM, and amplitudes ranging from 0.25 to 3 mM were delivered to islets while monitoring $[Ca^{2+}]_i$ changes within individual islets (Fig. 1 *B*). $[Ca^{2+}]_i$ is a good marker for insulin secretion because they are proportional (32,33). We observed slow oscillations of $[Ca^{2+}]_i$ with a period of ~ 5 min, but not faster oscillations because the imaging rate was 0.05 Hz. To illustrate entrainment, the phase angles (Φ) between each glucose and $[Ca^{2+}]_i$ oscillation from four experiments are shown on the polar plot in Fig. 1 *C*. Entrainment is evident by convergence of Φ at a

particular value, as illustrated by the blue, black, and green points in Fig. 1 *C*. As shown by the red points, Φ did not converge for each condition tested, which is discussed below.

To better quantify entrainment, a synchronization index (λ) was employed (25,30,31). λ indicates the degree of synchrony between the imposed glucose oscillations and the resulting oscillations of $[Ca^{2+}]_i$ with values of λ near 1 indicating complete synchronization. λ was calculated for all islets (n = 89) at each combination of glucose amplitude and period tested (188 conditions tested). The results of the experiments are shown in Fig. 1 *D* with the forcing glucose amplitude on the ordinate and the ratio of the forcing period to the islet's natural period (T_f/T_n) on the abscissa. Islets were deemed entrained if $\lambda \geq 0.7$ (blue circles) whereas $\lambda < 0.7$ indicates no entrainment (red crosses). Entrainment was achieved provided that the forcing amplitude was sufficiently large, as expected in entrainment experiments (34,35).

Closed-loop experiments using a model of insulin-dependent glucose uptake

After determining the region of entrainment for islets, the feedback loop was closed (Fig. 2) by stimulating groups of 5 to 10 islets with glucose while measuring $[Ca^{2+}]_i$ changes within each islet. The $[Ca^{2+}]_i$ from all islets was averaged (Ca_{avg}) and was converted into a measure of insulin secretion in arbitrary units (I_{avg}). Based on previous findings (32,33), this was modeled as an increasing linear function above a threshold value (Ca_{thr}) of Ca_{avg} (19):

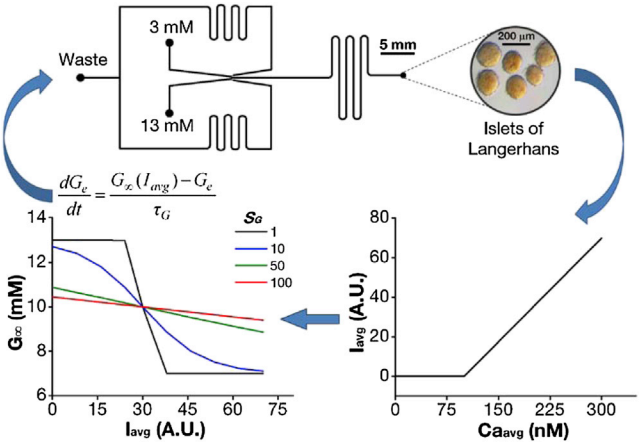

FIGURE 2 Overview of closed-loop feedback system. Beginning from the top left, a microfluidic device produced varying concentrations of glucose and delivered to batches of 5 to 10 islets shown in the inset. $[Ca^{2+}]_i$ from individual islets is measured using Fura-2 and the average calcium level of the population (Ca_{avg}) is converted to an average insulin secretion level (I_{avg}; arbitrary units) using a linear proportionality (*bottom right*). I_{avg} is the sole input to the asymptotic glucose response function, G_∞ (*bottom left*). Using G_∞, the extracellular glucose level (G_e) is delivered to the islets at a rate defined by τ_G. This new G_e value would induce a new Ca_{avg} that closes the feedback loop.

$$I_{avg}(Ca_{avg}) = \begin{cases} I_{slope}(Ca_{avg} - Ca_{thr}) & for\ Ca_{avg} \geq Ca_{thr} \\ 0 & for\ Ca_{avg} < Ca_{thr} \end{cases} \quad (3)$$

$$Ca_{thr} = (Ca_{max} - Ca_{min})\kappa + Ca_{min} \quad (4)$$

The parameters I_{slope} and κ were set at 1 A.U.*nM^{-1} and 0.1, respectively, and Ca_{max} and Ca_{min} were dependent on the individual experiment. Although a sigmoidal fit could have been used to model I_{avg} *vs.* Ca_{avg}, the $[Ca^{2+}]_i$ and insulin correlation is nearly linear within the $[Ca^{2+}]_i$ ranges we observed (32). That is, the $[Ca^{2+}]_i$ is in the linear portion of the sigmoidal curve over the ranges we observed. The asymptotic glucose response function G_∞ was modeled as a decreasing sigmoidal function of I_{avg} (Fig. 2), given by the following:

$$G_\infty(I_{avg}) = G_{min} + \frac{G_{min} - G_{max}}{1 + \exp[(I_{avg} - I_{1/2})/S_G]} \quad (5)$$

$I_{1/2}$ is the point of inflection of the curve and is the point at which G_∞ is midway between G_{min} and G_{max}, S_G is the steepness parameter of the curve, and parameters G_{min} and G_{max} were the minimum and maximum glucose levels of the curve and were set to 7 and 13 mM, respectively.

The extracellular glucose concentration (G_e) was updated using the following differential equation:

$$\frac{dG_e}{dt} = \frac{G_\infty(I_{avg}) - G_e}{\tau_G} \quad (6)$$

This differential equation was discretized as described in the Materials and Methods section, Eq. 1. All parameters and variables are shown in Tables 1 and 2, respectively. In this model, two key parameters shaped the timing and magnitude of the feedback response. Parameter S_G adjusted G_∞, with large values producing a low sensitivity, i.e., a shallow glucose response to I_{avg} (Fig. 2). Parameter τ_G was the time constant for the feedback response, with large values of τ_G

TABLE 1 Parameters and values used in the experiments

Parameter	Description	Value
I_{slope}	Slope of Ca_{avg} to I_{avg} conversion	1 A.U.*nM^{-1}
Ca_{thr}	Threshold $[Ca^{2+}]_i$ for insulin release	83-105 nM
Ca_{min}	Minimum $[Ca^{2+}]_i$	70-90 nM
Ca_{max}	Maximum $[Ca^{2+}]_i$	200-240 nM
κ	Fraction above Ca_{min} to set Ca_{thr}	0.1
G_{min}	Minimum glucose value of G_∞	7 mM
G_{max}	Maximum glucose value of G_∞	13 mM
$I_{1/2}$	Inflection point of G_∞	30-40 A.U.
S_G	Steepness of G_∞ (smaller is steeper)	0.1, 1, 10, 50, 100 A.U.
τ_G	Time constant for feedback response	50, 300, 450, 600, 900 s

Values that are shown as a range varied between experiments depending on the islets examined.

TABLE 2 Variables used in the experiments

Parameter	Description	Unit
Ca_{avg}	Average $[Ca^{2+}]_i$ measured every 20 s	nM
I_{avg}	Average insulin secretion	A.U.
G_∞	Asymptotic glucose response function	mM

producing a slow feedback response. Experiments were performed using S_G values of 0.1, 1, 10, 50, and 100 and τ_G values of 50, 300, 450, 600, and 900 s.

A group of 10 islets was initially stimulated with a constant 10 mM glucose (Fig. 3 *A*, red line) which induced uncoordinated $[Ca^{2+}]_i$ oscillations among islets. The color density map at the bottom of Fig. 3 *A* shows that all islets responded to the increased glucose with $[Ca^{2+}]_i$ oscillations, but these oscillations were out of phase. Accordingly, the Ca_{avg} response (black line) did not exhibit coherent rhythmicity. After 46 min, the extracellular glucose level was adjusted dynamically, as described above, closing the feedback loop. With the parameter values used in Fig. 3 *A* ($S_G = 1$, $\tau_G = 50$ s), the individual islets synchronized as evident by the vertical stripes in the color density map. Oscillations in both Ca_{avg} and the extracellular glucose level were produced with a period of 4.7 and 4.8 min, respectively. The insulin concentration (Fig. 3 *A*, blue curve) was measured simultaneously with $[Ca^{2+}]_i$ and a similar rhythmic pattern was observed (4.9 min), and was in phase with Ca_{avg}. Fura-2 ratiometric images of the islet population from different times are shown in Figs. 3 *B* and *C*. The images in Fig. 3 *B* were taken at two points during the delivery of constant glucose and show heterogeneous $[Ca^{2+}]_i$ values for the different islets, indicating that the islets were unsynchronized. In Fig. 3 *C*, the images were acquired when the feedback was on, and show a homogeneous $[Ca^{2+}]_i$ as would be expected from a synchronized population of islets. The movie that the images in Fig. 3 *B* and *C* were taken is provided in the Supporting Material (Movie S1).

To examine how the dynamic glucose feedback varied with the two feedback parameters, other combinations of S_G and τ_G were used and representative experiments are shown in Fig. 4 *A–D*. For the same S_G, increasing τ_G decreased the overall glucose amplitude. For example, Fig. 4 *A* shows an experiment that used five islets with parameters $S_G = 10$, $\tau_G = 50$ s and produced ~ 2 mM amplitude glucose oscillations with large amplitude oscillations in Ca_{avg} indicating the islets were synchronized ($\lambda = 0.97$). In Fig. 4 *B*, five different islets were used with $S_G = 10$, $\tau_G =$ 600 s. No pulsatility in Ca_{avg} was apparent and the glucose level was relatively flat, indicating that the islets were not synchronized ($\lambda = 0.33$).

Figs. 4 *C* and *D* show representative results of the effect of S_G on synchronization. In Fig. 4 *C*, six islets were used with parameters $S_G = 50$, $\tau_G = 50$ s, and in Fig. 4 *D*, eight islets were used with $S_G = 100$, $\tau_G = 50$ s. Synchronization only occurred with the smaller S_G value ($\lambda = 0.93$ and 0.53 for Fig. 4 *C* and *D*, respectively). The effects of S_G and τ_G on the average λ and average induced glucose amplitudes are summarized in Fig. 4 *E*. The shapes of the points indicate values of τ_G, whereas the colors indicate values of S_G, with error bars corresponding to +/− 1 standard deviation.

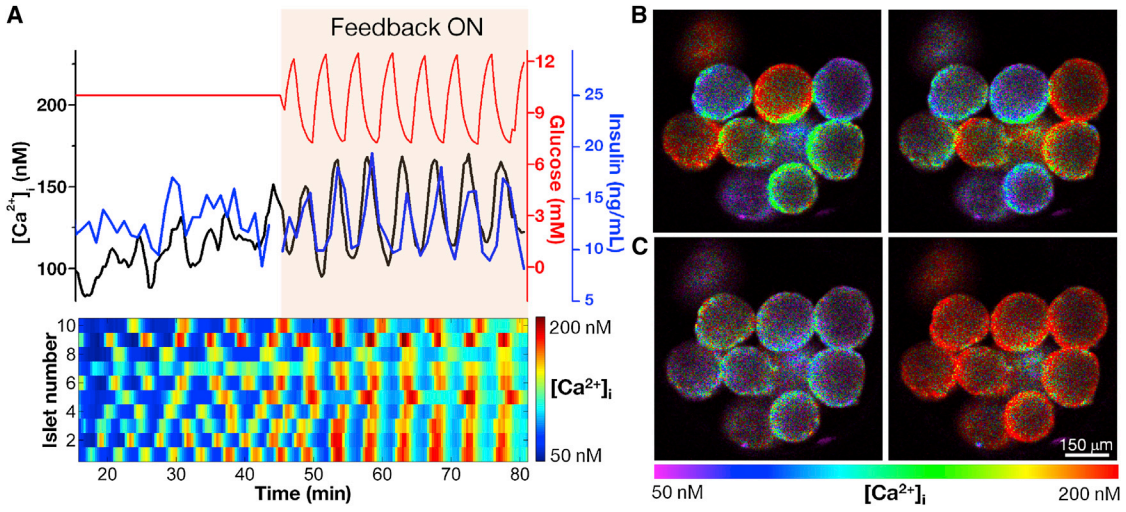

FIGURE 3 Islet synchronization occurs when the feedback loop is closed. (*A*) In this example, the feedback loop was closed using parameter values of $S_G = 1$, $\tau_G = 50$ s with 10 islets in the microfluidic chamber. At time 46 min, the feedback was turned on and G_e changed in response to Ca_{avg}. The glucose level is shown at the top in red, whereas Ca_{avg} (*black line*) and insulin (*blue line*) are shown below the glucose. The $[Ca^{2+}]_i$ from all islets is shown in the color density map at the bottom. Scale bars for all measurements are shown adjacent to the graphs. (*B*) Two fluorescent ratiometric images of Fura-2 taken of the islets shown in part *A* before the onset of feedback. The image on the left was taken at time 25 min and the one on the right at 32 min. (*C*) The two images correspond to times 51 min (*left*) and 63 min (*right*), when feedback was on. The color scale bar for *B* and *C* are shown below *C*.

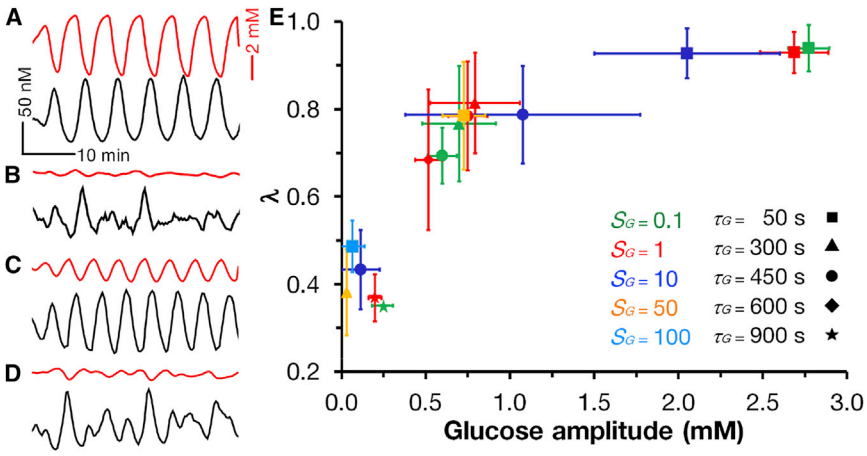

FIGURE 4 Glucose amplitudes and islet synchronization indices (λ) as a function of S_G and τ_G during the closed-loop feedback experiments. (*A* to *D*) In each trace, the glucose concentration (*red*) is shown above the Ca_{avg} trace (*black*). Different traces correspond to different parameter values in the feedback system. (*A*) $S_G = 10$ and $\tau_G = 50$ s; (*B*) $S_G = 10$ and $\tau_G = 600$ s; (*C*) $S_G = 50$ and $\tau_G = 50$ s; and (*D*) $S_G = 100$ and $\tau_G = 50$ s. In traces *A* and *C*, the islet population was synchronized (λ= 0.97 (five islets) and 0.93 (six islets), respectively). With the large τ_G value in *B* and the large S_G value in *D*, the amplitudes of the glucose oscillations were small and islets were not synchronized (λ = 0.33 (five islets) and 0.53 (eight islets), respectively). (*E*) The average λ are shown versus the average glucose amplitude that resulted from the feedback interactions for all experiments. The colors and shapes of the data points correspond to the values of S_G and τ_G as shown in the legend and error bars correspond to +/− 1 standard deviation. At low values of S_G and τ_G, glucose amplitudes > 0.4 mM are produced and the islets synchronize (high λ).

DISCUSSION

We set out to test the hypothesis that a dynamic interaction between the pancreas and liver could synchronize the oscillations of activity and insulin secretion across an islet population (19). By taking up glucose, the liver provides negative feedback onto islets, all of which sense the glucose level and respond accordingly. The result of this negative feedback would be both oscillations of insulin and glucose, both of which have been observed in vivo (1,2,7–9,24). Initial tests of the hypothesis were performed in an open-loop manner to verify that glucose oscillations of appropriate period and amplitude, here imposed on the islets, could indeed entrain oscillations in the islet Ca^{2+} concentration. Similar experiments have been performed with single (20,26,36) and groups (25,37,38) of islets, but the ranges of glucose periods and amplitudes were not investigated. We found that islets were entrained by sinusoidal glucose levels with periods near the natural oscillation period and with glucose amplitudes above 0.5 mM. It has been reported that even small amplitude oscillations of glucose (~ 0.3 mM, or 5%) (39) entrains in vivo pulses of insulin, and our results are similar in this manner. Recent work also demonstrates that islets can be entrained at harmonics of the glucose oscillation, so that a 10 min glucose wave can entrain two pulses of $[Ca^{2+}]_i$ (38). We too observed a range of harmonics, ranging from 3:1 to 1:2 but only show the 1:1 entrainment in Fig. 1 *A*.

After confirmation that islets can be entrained to glucose oscillations with the appropriate combinations of amplitudes and periods, the closed-loop experiments were performed where the response of the islet population was used to update the glucose level, via Eqs. 3 to 6, to be delivered to the islets. The two parameters we tested, S_G and τ_G, were based on liver glucose absorption and the time the new glucose level was delivered to the islets, respectively. Because physiological values are not known for these parameters, a range of values was tested. As shown in Fig. 3, insulin release and Ca_{avg} became synchronized with a concomitant production of oscillatory glucose levels using the appropriate model parameters. In all closed-loop experiments performed, the glucose concentration was 180° out of phase with both insulin and Ca_{avg}. This phase difference is attributable to the asymptotic glucose response function and was also observed when this dynamic feedback interaction was mathematically modeled (see Fig. 10 of (19)). Fig. 3 also confirms that the use of Ca_{avg} is a suitable marker for I_{avg} in later experiments because oscillations of insulin and Ca_{avg} were in phase.

The oscillations seen in Fig. 3 *A* in the glucose trace, color density map, and the Ca_{avg} trace were the result of mutual interactions between the islets in the microfluidic chamber and the dynamic glucose feedback. That is, with the glucose feedback action, the majority of islets in the chamber synchronized their activity to produce a rhythm whose period was determined by the intrinsic oscillatory periods of the islet population. As expected, the amplitude and period of the glucose oscillation were within the entrainment window measured in the open-loop experiments (Fig. 1 *D*).

The ranges of τ_G and S_G that produced a synchronized population were explored, and it was found that increasing either τ_G or S_G produced a decrease in the glucose amplitude with a concomitant drop in λ. With large values of S_G ($\geq$ 100), the glucose response function was too flat to reflect changes in I_{avg} and the islets did not synchronize. With large values of τ_G the rate of response of the feedback system was reduced and the extreme values of the response function (G_{max} and G_{min}) were never reached, reducing the amplitude of the glucose oscillations. As shown by Fig. 4 *E*, it was essential for the amplitude of the glucose oscillations to be > ~ 0.4 mM. Combinations of S_G and τ_G that produced glucose amplitudes between 0.40 to 3 mM were successful at synchronizing islet populations ($\lambda \geq 0.7$), but below

0.40 mM were not. These results are consistent with the open-loop experiments in which glucose oscillations were imposed; amplitudes below 0.5 mM were largely outside of the islet entrainment window (Fig. 1 *D*).

Although our dynamic glucose model is simple, it captures the key element of negative feedback provided by the liver, and results in islet oscillations with a period similar to those observed in vivo (1–3,7–9). For combinations of S_G and τ_G that produced $\lambda \geq 0.7$, the Ca_{avg} and glucose oscillation periods were within the range of 5 to 8 min. This is important because it is what would be expected if the rhythmicity were attributable to the intrinsic period of the islets, rather than the glucose feedback system. The liver is known to take up 25% to 35% of an oral glucose load (40–42) with blood circulation taking ~ 1 min. Combined with the inhibitory effect of insulin on hepatic glucose production, the liver has the capability of making large changes in the blood glucose level and the effects of these changes can be rapid.

Negative feedback provided by the liver is not the only plausible mechanism for islet synchronization. Intrapancreatic ganglia could provide pacemaking activity to entrain islet oscillations (10,17,43), but at present there are no data suggesting that ganglia neurons exhibit coordinated pacemaking activity. It is also possible that islets communicate through chemical messengers in a paracrine fashion, and this would account for observations of pulsatile insulin in the perfused pancreas (23,44,45) and from superfused islets (46,47). However, no such paracrine factor has been isolated, and we find no coordination of islet activity with a constant glucose level (Fig. 3). Given the physiological importance of insulin pulsatility, it is likely that there are overlapping mechanisms for synchronization, and indeed, no one mechanism can explain all the reports of synchronization in different preparations. Our data support the hypothesis that a dynamic interaction between the pancreas and the liver could synchronize intrinsic islet oscillations, and can provide one mechanism for islet synchronization in a number of species, including humans.

SUPPORTING MATERIAL

One movie is available at http://www.biophysj.org/biophysj/supplemental/S0006-3495(14)00398-1.

R. B. and M. G. R. were partially supported from NIH grant DK080714.

The authors declare no conflict of interest.

REFERENCES

1. Song, S. H., S. S. McIntyre, …, P. C. Butler. 2000. Direct measurement of pulsatile insulin secretion from the portal vein in human subjects. *J. Clin. Endocrinol. Metab.* 85:4491–4499.
2. Nunemaker, C. S., D. H. Wasserman, …, L. S. Satin. 2006. Insulin secretion in the conscious mouse is biphasic and pulsatile. *Am. J. Physiol. Endocrinol. Metab.* 290:E523–E529.
3. Matveyenko, A. V., D. Liuwantara, …, P. C. Butler. 2012. Pulsatile portal vein insulin delivery enhances hepatic insulin action and signaling. *Diabetes.* 61:2269–2279.
4. O'Rahilly, S., R. C. Turner, and D. R. Matthews. 1988. Impaired pulsatile secretion of insulin in relatives of patients with non-insulin-dependent diabetes. *N. Engl. J. Med.* 318:1225–1230.
5. Schmitz, O., N. Pørksen, …, S. M. Pincus. 1997. Disorderly and nonstationary insulin secretion in relatives of patients with NIDDM. *Am. J. Physiol.* 272:E218–E226.
6. Gilon, P., R. M. Shepherd, and J.-C. Henquin. 1993. Oscillations of secretion driven by oscillations of cytoplasmic Ca^{2+} as evidences in single pancreatic islets. *J. Biol. Chem.* 268:22265–22268.
7. Matveyenko, A. V., J. D. Veldhuis, and P. C. Butler. 2008. Measurement of pulsatile insulin secretion in the rat: direct sampling from the hepatic portal vein. *Am. J. Physiol. Endocrinol. Metab.* 295:E569–E574.
8. Pørksen, N., S. Munn, …, P. Butler. 1995. Pulsatile insulin secretion accounts for 70% of total insulin secretion during fasting. *Am. J. Physiol.* 269:E478–E488.
9. Goodner, C. J., F. G. Hom, and D. J. Koerker. 1982. Hepatic glucose production oscillates in synchrony with the islet secretory cycle in fasting rhesus monkeys. *Science.* 215:1257–1260.
10. Ahrén, B. 2000. Autonomic regulation of islet hormone secretion—implications for health and disease. *Diabetologia.* 43:393–410.
11. Hellman, B., H. Dansk, and E. Grapengiesser. 2004. Pancreatic β-cells communicate via intermittent release of ATP. *Am. J. Physiol. Endocrinol. Metab.* 286:E759–E765.
12. Ahrén, B., G. J. Taborsky, Jr., and D. Porte, Jr. 1986. Neuropeptidergic versus cholinergic and adrenergic regulation of islet hormone secretion. *Diabetologia.* 29:827–836.
13. Brunicardi, F. C., D. M. Shavelle, and D. K. Andersen. 1995. Neural regulation of the endocrine pancreas. *Int. J. Pancreatol.* 18:177–195.
14. Berthoud, H. R., and T. L. Powley. 1990. Identification of vagal preganglionics that mediate cephalic phase insulin response. *Am. J. Physiol.* 258:R523–R530.
15. Kirchgessner, A. L., and M. D. Gershon. 1990. Innervation of the pancreas by neurons in the gut. *J. Neurosci.* 10:1626–1642.
16. King, B. F., J. A. Love, and J. H. Szurszewski. 1989. Intracellular recordings from pancreatic ganglia of the cat. *J. Physiol.* 419:379–403.
17. Fendler, B., M. Zhang, …, R. Bertram. 2009. Synchronization of pancreatic islet oscillations by intrapancreatic ganglia: a modeling study. *Biophys. J.* 97:722–729.
18. Grapengiesser, E., H. Dansk, and B. Hellman. 2004. Pulses of external ATP aid to the synchronization of pancreatic β-cells by generating premature Ca^{2+} oscillations. *Biochem. Pharmacol.* 68:667–674.
19. Pedersen, M. G., R. Bertram, and A. Sherman. 2005. Intra- and inter-islet synchronization of metabolically driven insulin secretion. *Biophys. J.* 89:107–119.
20. Sturis, J., W. L. Pugh, …, K. S. Polonsky. 1994. Alterations in pulsatile insulin secretion in the Zucker diabetic fatty rat. *Am. J. Physiol.* 267:E250–E259.
21. Pørksen, N. 2002. The in vivo regulation of pulsatile insulin secretion. *Diabetologia.* 45:3–20.
22. Goodner, C. J., D. J. Koerker, …, E. Samols. 1991. In vitro pancreatic hormonal pulses are less regular and more frequent than in vivo. *Am. J. Physiol.* 260:E422–E429.
23. Gilon, P., M. A. Ravier, …, J.-C. Henquin. 2002. Control mechanisms of the oscillations of insulin secretion in vitro and in vivo. *Diabetes.* 51 (*Suppl.*):S144–S151.
24. Lang, D. A., D. R. Matthews, …, R. C. Turner. 1979. Cyclic oscillations of basal plasma glucose and insulin concentrations in human beings. *N. Engl. J. Med.* 301:1023–1027.
25. Zhang, X., A. Daou, …, M. G. Roper. 2011. Synchronization of mouse islets of Langerhans by glucose waveforms. *Am. J. Physiol. Endocrinol. Metab.* 301:E742–E747.

26. Zhang, X., A. Grimley, …, M. G. Roper. 2010. Microfluidic system for generation of sinusoidal glucose waveforms for entrainment of islets of Langerhans. *Anal. Chem.* 82:6704–6711.

27. Zhang, X., and M. G. Roper. 2009. Microfluidic perfusion system for automated delivery of temporal gradients to islets of Langerhans. *Anal. Chem.* 81:1162–1168.

28. Ferry, M. S., I. A. Razinkov, and J. Hasty. 2011. Microfluidics for synthetic biology: from design to execution. *Methods Enzymol.* 497:295–372.

29. Grynkiewicz, G., M. Poenie, and R. Y. Tsien. 1985. A new generation of Ca^{2+} indicators with greatly improved fluorescence properties. *J. Biol. Chem.* 260:3440–3450.

30. Zarkovic, M., and J.-C. Henquin. 2004. Synchronization and entrainment of cytoplasmic Ca^{2+} oscillations in cell clusters prepared from single or multiple mouse pancreatic islets. *Am. J. Physiol. Endocrinol. Metab.* 287:E340–E347.

31. Rosenblum, M., A. Pikovsky, …, P. A. Tass. 2001. Phase synchronization: from theory to data analysis. *In* Neuro-Informatics and Neural Modelling. F. Moss and S. Gielen, editors. Elsevier, Amsterdam, pp. 279–321.

32. Jonas, J.-C., P. Gilon, and J.-C. Henquin. 1998. Temporal and quantitative correlations between insulin secretion and stably elevated or oscillatory cytoplasmic Ca^{2+} in mouse pancreatic β-cells. *Diabetes.* 47:1266–1273.

33. Nunemaker, C. S., J. F. Dishinger, …, L. S. Satin. 2009. Glucose metabolism, islet architecture, and genetic homogeneity in imprinting of $[Ca^{2+}]_i$ and insulin rhythms in mouse islets. *PLoS ONE.* 4:e8428.

34. Pikovsky, A., M. Rosenblum, and J. Kurths. 2001. Synchronization: A Universal Concept in Nonlinear Sciences. Cambridge University Press, Cambridge, MA.

35. Mondragón-Palomino, O., T. Danino, …, J. Hasty. 2011. Entrainment of a population of synthetic genetic oscillators. *Science.* 333:1315–1319.

36. Chou, H. F., and E. Ipp. 1990. Pulsatile insulin secretion in isolated rat islets. *Diabetes.* 39:112–117.

37. Zhang, X., R. Dhumpa, and M. G. Roper. 2013. Maintaining stimulant waveforms in large-volume microfluidic cell chambers. *Microfluid. Nanofluid.* 15:65–71.

38. Pedersen, M. G., E. Mosekilde, …, D. S. Luciani. 2013. Complex patterns of metabolic and Ca^{2+} entrainment in pancreatic islets by oscillatory glucose. *Biophys. J.* 105:29–39.

39. Pørksen, N., C. Juhl, …, O. Schmitz. 2000. Concordant induction of rapid in vivo pulsatile insulin secretion by recurrent punctuated glucose infusions. *Am. J. Physiol. Endocrinol. Metab.* 278:E162–E170.

40. Moore, M. C., K. C. Coate, …, A. D. Cherrington. 2012. Regulation of hepatic glucose uptake and storage in vivo. *Adv. Nutr.* 3:286–294.

41. Ferrannini, E., O. Bjorkman, …, R. A. DeFronzo. 1985. The disposal of an oral glucose load in healthy subjects. A quantitative study. *Diabetes.* 34:580–588.

42. Mari, A., J. Wahren, …, E. Ferrannini. 1994. Glucose absorption and production following oral glucose: comparison of compartmental and arteriovenous-difference methods. *Metabolism.* 43:1419–1425.

43. Zhang, M., B. Fendler, …, L. Satin. 2008. Long lasting synchronization of calcium oscillations by cholinergic stimulation in isolated pancreatic islets. *Biophys. J.* 95:4676–4688.

44. Stagner, J. I., E. Samols, and G. C. Weir. 1980. Sustained oscillations of insulin, glucagon, and somatostatin from the isolated canine pancreas during exposure to a constant glucose concentration. *J. Clin. Invest.* 65:939–942.

45. Salehi, A., S. S. Qader, …, B. Hellman. 2005. Inhibition of purinoceptors amplifies glucose-stimulated insulin release with removal of its pulsatility. *Diabetes.* 54:2126–2131.

46. Hellman, B., A. Salehi, …, E. Grapengiesser. 2009. Glucose generates coincident insulin and somatostatin pulses and antisynchronous glucagon pulses from human pancreatic islets. *Endocrinology.* 150:5334–5340.

47. Hellman, B., A. Salehi, …, E. Gylfe. 2012. Isolated mouse islets respond to glucose with an initial peak of glucagon release followed by pulses of insulin and somatostatin in antisynchrony with glucagon. *Biochem. Biophys. Res. Commun.* 417:1219–1223.